



ELSEVIER

Available online at www.sciencedirect.com

SCIENCE @ DIRECT®

Nuclear Instruments and Methods in Physics Research A 507 (2003) 636–642

**NUCLEAR
INSTRUMENTS
& METHODS
IN PHYSICS
RESEARCH**
Section Awww.elsevier.com/locate/nima

Fast pulsed UV light source and calibration of non-linear photomultiplier response

M. Vicić^{a,*}, L.G. Sobotka^b, J.F. Williamson^a, R.J. Charity^b, J.M. Elson^b^aDepartment of Radiation Oncology, Washington University, 510 S. Kingshighway Blvd., St. Louis, MO 63110, USA^bDepartment of Chemistry, Washington University, St. Louis, MO 63130, USA

Received 20 August 2002; received in revised form 18 February 2003; accepted 8 March 2003

Abstract

A novel ultraviolet pulsed-light source with a digitally controlled amplitude has been developed and used to determine the response of the BURLE 8850 photomultiplier tube for light intensities close to that corresponding to single photoelectrons to those well beyond the linear response region.

© 2003 Elsevier Science B.V. All rights reserved.

PACS: 29.40.Mc; 85.60.Ha; 85.60.Jb

Keywords: Light pulser; Photomultiplier; Calibration; UV LED

1. Introduction

Utilization of pulsed-light sources for the calibration of photomultiplier tube (PMT) response is a well-established technique. The most common approach is to use a constant-amplitude pulsed source and a set of neutral density filters. The inherent drawback of this method is the relatively poor tolerance of the filters' absolute transmission coefficients τ ($\sim 5\%$ for most commercial models). In practice, one finds that filters need to be positioned with high mechanical precision in order to achieve highly reproducible results. This is due to the fact that internal reflections in the optical path significantly contribute to the overall light attenuation.

Alternative techniques involving calibrated light sources are also plagued with experimental difficulties, making calibration of a PMT both awkward and time consuming. A brief but informative review of the problems associated with the photomultiplier calibration can be found in Ref. [1].

While a linear response is often a desired characteristic of a PMT, operation in a non-linear mode is beneficial in experiments for which extended dynamical range is required. However, this approach necessitates even more precise knowledge of the photomultiplier response curve. For example, recent work by our group required calibration of a PMT from light levels less than that required to produce one photoelectron (p.e.) (on average) to levels for which the tube (and the base) clearly exhibited a non-linear response.

In order to provide the necessary calibration, we designed a novel ultraviolet (UV) light pulser with digitally controlled amplitude. The device is

*Corresponding author. Tel.: +1-314-362-2629; fax: +1-314-362-2682.

E-mail address: vica@castor.wustl.edu (M. Vicić).

self-calibrating without a priori knowledge of the light sensor response curve.

2. Light source

Light-emitting diodes (LEDs) have been successfully used for the fast light pulse applications by numerous authors (e.g. Refs. [2–4]). Our pulser is based on a relatively new, commercially available, Nichia model NSHU550E LED. This diode emits in the near UV, with the peak in the emission spectrum at 375 nm. A set of four LEDs illuminate an integrating hemisphere of UV transparent methyl methacrylate (Fig. 1). The hemisphere surface is covered with diffusive white reflector paint (Bicron BC-620). A rigid UV transparent light pipe (LP), optically coupled to the hemisphere, guides the light to the photomultiplier tube. The crucial assumption for this arrangement is that the light arriving to the PMT represents a linear superposition of the light intensities from individual LEDs. Moreover, the diffusive surface of the hemisphere randomizes photon trajectories, rendering the light distribution at the LP exit aperture homogenous and independent of the originating LED. Thus, if all four LEDs are simultaneously pulsed, the resultant amplitude is

$$A_r = \sum_{i=1}^4 A_i \quad (1)$$

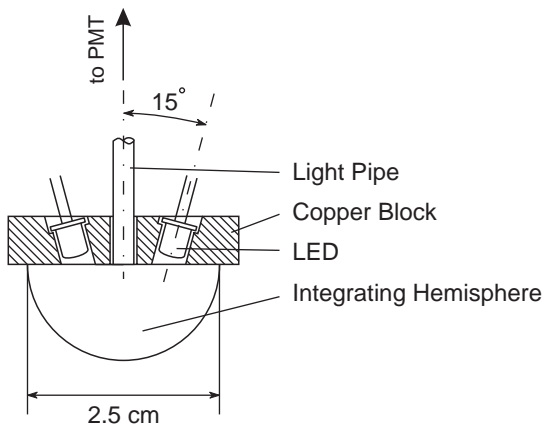


Fig. 1. Cross-sectional view of the light source. The other two LEDs are positioned in a plane perpendicular to the drawing.

where A_i represents amplitude at the exit of the LP when only the i th diode is pulsed. The individual relative amplitudes are tuned in the following sequence: $A_1 = 1$, $A_2 = 2$, $A_3 = 4$ and $A_4 = 8$. The electronic circuit that drives the LEDs (described in detail in the next section) provides the means of including or excluding any particular diode from the pulse. This inclusion–exclusion scheme can be represented as a four-bit binary number k . For the above choice of LED amplitudes, the resultant light output A_r is proportional to k . We propose the name “Digital to Light Converter” (DLC) for this kind of an arrangement.

3. Driving electronics

The production of high-speed (<10 ns) light pulses with sufficient amplitude from LEDs, imposes very stringent requirements on the driving circuitry. The LED represents a capacitive load with a typical intrinsic capacitance of few hundred pF in series with a resistance of approximately 10Ω [5]. We have adopted a variant of a design based on the avalanche transistor reported by several authors [3,6,7]. The schematic diagram of the driver is given in Fig. 2. The trimmer potentiometer labelled “Amp.” enables adjustment of the pulse amplitude. An electrical pulse width of 3.2 ns was obtained (measured at 5% of the maximum pulse amplitude). A digital oscilloscope was used for the comparison of the PMT pulses produced by a fast plastic scintillator (Bicron BC-400) exposed to a ^{137}Cs radioactive source and the pulses obtained from the same scintillator illuminated directly by the LED pulser. The comparison revealed no significant difference in the pulse width (~ 15 ns FWHM). Consequently, no attempt was made to “quench” the LED injection current by using inductors [3,6] or coaxial lines [7].

4. Temperature dependence of LED source

Semiconductor light sources are notoriously sensitive to temperature variations. Our preliminary measurements showed that the model

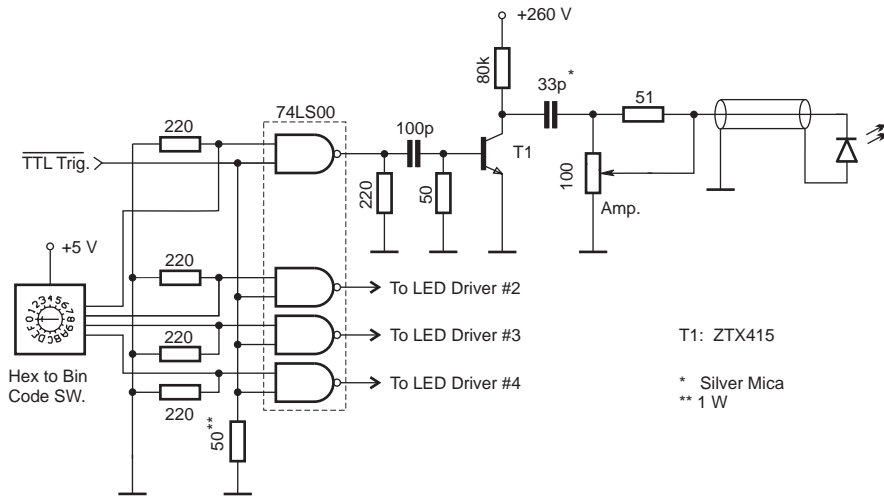


Fig. 2. Schematic diagram of the LED driving electronics.

NSHU550E LED is particularly troublesome in this respect, with the temperature coefficient approaching $2.2\%/^{\circ}\text{C}$. The diodes were mounted in a copper block (Fig. 1), along with a sensitive thermistor. The thermal resistance between the copper and the diodes' metal housing was further reduced by use of a silver-bearing silicon thermal compound. A 50 W Peltier thermoelectric cooler (TEC) was attached to the copper block. The other side of the TEC was attached to a massive high-efficiency heatsink. The whole assembly (excluding heatsink) is immersed in expanded polyurethane foam. The temperature of the LEDs is controlled by a high-precision Proportional-Integral-Derivative (PID) controller. The temperature stability achieved at the sensor was $\pm 0.01^{\circ}\text{C}$ at 18°C . A slight dependence of the light intensity was observed with the varying frequency of the pulsing. This suggests that the temperature gradients between LEDs' p-n junctions and the copper block are still present, limiting the frequency range of the pulser's calibrated operation.

5. Measurements

With the experimental setup represented in Fig. 3, we performed the calibration of the pulser

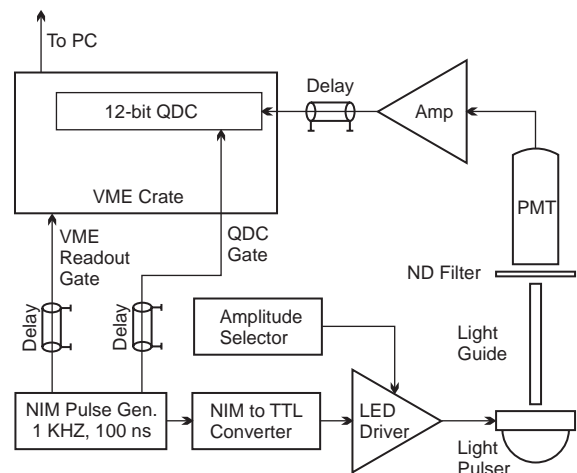


Fig. 3. Block diagram of the experimental setup.

as well as a series of response curve measurements for the BURLE 8850 photomultiplier.

5.1. Calibration

In order to calibrate the LED amplitudes in a binary sequence, we employed the following procedure: LED 1 was set to an arbitrary low amplitude A_1 . The amplitude of LED 4 was tuned to match ($A_4 = A_1$). The matching was done by

comparing the PMT pulse-height spectra recorded separately for diodes 1 and 4. By simultaneous pulsing of LED 1 and LED 4, a new spectrum corresponding to the $2A_1$ was recorded. The amplitude of LED 2 was then tuned to match this spectrum. Simultaneous firing of LEDs 1,2 and 4 now produces pulses of amplitude $4A_1$. This pulse-height spectrum was used for tuning of LED 3. Finally, firing of all four LEDs enabled recording of an $8A_1$ spectrum, which was used to tune LED 4 to its final value. This “bootstrap” calibration of the pulser does not assume linearity of the PMT, only that its response curve is monotonic.

An additional independent measurement was made to verify the initial assumption of the linear additivity Eq. (1). We used a silicon PIN diode (Hamamatsu S3590-03) as the light sensor. The diode was attached to the digital electrometer (Keithley model 6517). The electrometer also served as a DC bias source (30 V) for the diode. In order to minimize a dark current, the PIN diode was cooled with a dry ice. The measured dark current was 1.2×10^{-13} A. To obtain a signal well above the noise floor, the pulser was operated at the frequency of 100 kHz. This is a two orders of magnitude higher duty cycle compared to the frequency at which the pulser was calibrated (1 kHz). The results of the measurements for the three most significant bits of the pulser are presented in Table 1. The third column of the table I_{theor} represents a theoretical current values obtained by the summation of the measured currents for the individual LEDs (i.e. $I_{\text{theor}}(6) =$

$I(2) + I(4)$, $I_{\text{theor}}(10) = I(2) + I(8)$, $I_{\text{theor}}(12) = I(4) + I(8)$ and $I_{\text{theor}}(14) = I(2) + I(4) + I(8)$). The estimated error for the current readings is $\leq 1\%$ according to the manufacturer’s specifications. It is immediately obvious that the ratio $2 \div 4 \div 8$ of the intensities for the LEDs 2, 4 and 8, respectively is not preserved. This is easily explained by the fact that LEDs operate at the drastically higher duty cycle compared to the regime at which they were calibrated. On the other hand additivity (Eq. (1)) is demonstrated by these data. The comparison of the $I_{\text{theor}}(k)$ and the measured values of $I(k)$ for combinational values of k ($k = 6, 10, 12, 14$) reveals agreement within 1%, consistent with the experimental error.

5.2. Photomultiplier response curves

For very low light intensities, i.e. when each light pulse produces about 1 p.e. on average, the pulse-height distribution of a PMT is non-Gaussian and exhibits structure if single p.e. resolution exists. The interpretation of such spectra and the extraction of a quantitative measure of the incident light intensity presents a difficult problem that has been investigated by numerous authors [2,8–10]. Generally, the photomultiplier’s anode charge or pulse-height distribution $f(q - q_p)$ is modelled as

$$f(q - q_p) = \sum_{n=0}^{\infty} \frac{\mu^n}{n!} e^{-\mu} f_n(q - q_p) \tag{2}$$

where q is the PMT’s anode charge, q_p is the pedestal position, f_n denotes the normalized anode charge distribution when exactly n p.e.’s are emitted from the photocathode and μ is an average number of p.e.’s produced by the incident light pulse.

Eq. (2) is based on the assumption that constant amplitude light pulses liberate a Poisson distribution of p.e.’s from the cathode [11]. The exact form of f_n varies from model to model, but generally, for higher values of n , f_n is approximated by Gaussians centered at $n(q_0 - q_p)$, with the standard deviations proportional to $\sigma_0 \sqrt{n}$, where q_0 and σ_0 are quantities dependent on the PMT operating parameters.

Table 1
Measured current of the PIN diode as a function of the pulser channel k

k	$I(k)$ (10^{-11} A)	$I_{\text{theor}}(k)$ (10^{-11} A)	$\frac{I_{\text{theor}}(k) - I(k)}{I(k)}$
2	0.487		
4	1.423		
6	1.890	1.910	0.011
8	2.040		
10	2.534	2.539	0.002
12	3.442	3.475	0.010
14	3.914	3.950	0.009

Results are presented with the dark current subtracted.

In order to determine the light intensity, the measured pulse-height spectra can be fitted with the function: $B \cdot f(q, \mu, x_0, \sigma_0, p_i)$, where B represents the amplitude and μ, x_0, σ_0, p_i are fitting parameters. The set of parameters p_i is model specific (see the appendix). Parameter μ represents the average number of p.e.'s liberated per light pulse and is the sought-after measure of light intensity.

Ideally, a simple averaging of the measured spectrum can be used to determine the relative light intensity:

$$\bar{q} = \frac{\sum_{i=1}^{i_{\max}} (q_i - q_p) N_i}{\sum_{i=1}^{i_{\max}} N_i} \quad (3)$$

where i enumerates channels, and N_i represents the corresponding number of counts in that channel. However, in order to have $\bar{q} \propto \mu$, it is necessary that the measured spectrum contains the $n = 0$ (“pedestal”) events. Unfortunately, in the majority of experiments, the data acquisition trigger is derived from the discriminated PMT signal, thus the data set excludes pedestal events. As our experimental setup is driven by an external trigger, both measures of light intensity μ and \bar{q} , extracted from Eqs. (2) and (3), respectively, can be obtained.

The spectra shown in Fig. 4 were recorded for the pulser’s lowest three amplitude settings ($k = 1, 2, 3$) and with a high-attenuation neutral density filter inserted in the optical path. For $k = 1$, the first four p.e. peaks are clearly resolved because of the extremely high gain of the first dynode of the BURLE 8850 “Quantacon” photomultiplier tube.

The spectra were fitted with Eq. (2) using the response model described in the appendix. For the $k = 1$ spectrum, all fitting parameters of the model were kept free. For the spectra corresponding to $k = 2$ and 3, only B and μ were fit with the remaining parameters fixed to values derived from the $k = 1$ fit.

In order to determine the response function of the PMT for a fixed anode voltage ($V_a = 2750$ V), two sets of measurements were performed. Average anode charges $\bar{q}(k')$ (optical attenuator in place) and $\bar{q}(k'')$ (optical attenuator removed) were determined using Eq. (3). The PMT response

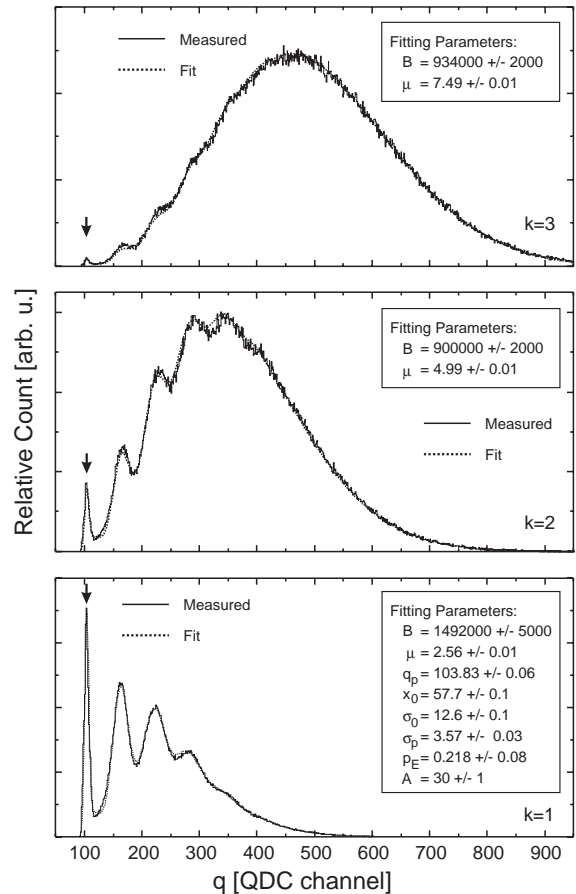


Fig. 4. Pulse-height spectra for the lowest three intensity settings of a digital to light converter. Vertical arrows indicate the pedestal position. See text for the definition of the parameters given in the insets.

function in the low light level range is shown in Fig. 5. As expected, the photomultiplier tube exhibits a linear behavior within experimental error.

For the first three values of k' , we have also determined the average number μ of p.e.'s by fitting the corresponding pulse-height spectra with Eq. (2). A comparison of the two methods for determining the light intensity is presented in Table 2. The ratios $\bar{q}(k')/\mu(k')$ are constant within 0.5%, signifying excellent agreement between these two methods.

The photomultiplier’s response for the higher light levels is presented in Fig. 6. In order to put both sets k' and k'' on the same scale and

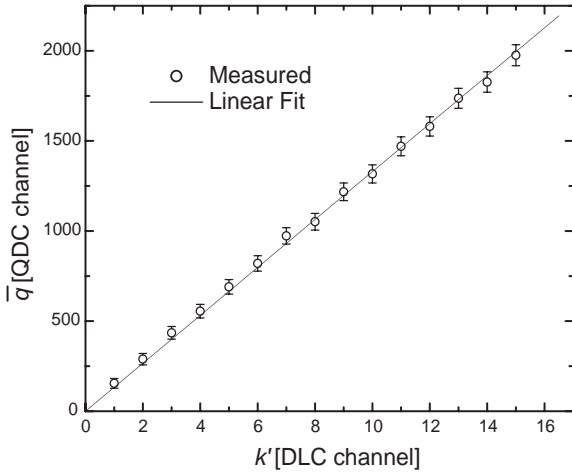


Fig. 5. PMT response curve in the low light level range. The error bars are the standard error of the mean.

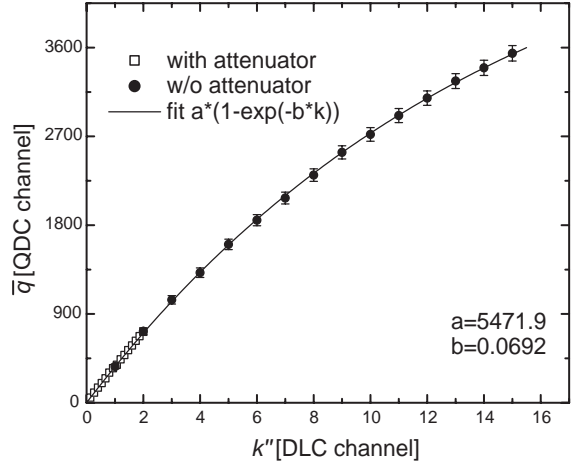


Fig. 6. PMT response curve at higher light intensities. The error bars are the standard error of the mean.

Table 2
Light intensities derived by averaging (\bar{q}) and fitting (μ)

k'	\bar{q}	μ	\bar{q}/μ
1	131.94	2.56	51.44
2	258.11	4.99	51.70
3	385.97	7.49	51.53

simultaneously obtain the response function, we performed an additional fitting procedure. The PMT response curve was assumed to be in the simple exponential form

$$\bar{q}(k) = a(1 - e^{-bk}). \tag{4}$$

The ratio of the high level to the attenuated light intensities, $g = k''/k'$, is not known a priori with sufficient accuracy, as it depends on the absolute transmission τ of the neutral density filter. The two sets of data were placed on the same scale by putting $k = k'/g$ for the first set and $k = k''$ for the second and including g in the set of fitting parameters. Using Eq. (4) both data sets were fitted simultaneously.

From Fig. 6 it is obvious that the “Quantacon” PMT exhibits non-linearities for the modest-sized light pulses of the present study. This is the price paid for the excellent single p.e. resolution.

6. Conclusions

Users of PMTs often wish to extract results at very low light levels and yet maintain a large dynamic range. These objectives are usually in conflict as achieving single p.e. sensitivity and resolution (1 p.e. from 2 p.e. and so on) requires high gain on the early dynodes which leads to space-charge-induced non-linearities for large light pulses. However, both experimental objectives can be attained if a means exists to calibrate the PMT response from very low light levels (defined as when the zero p.e. response is non-negligible) up to light levels which exhibit saturation effects. We have described a pulser system and an analysis scheme which accomplishes this. The pulser is self-calibrating and has digitally controlled amplitude, while the analysis scheme involves multiple folding of the PMT single p.e. response. In the case studied, the BURLE 8850 “Quantacon” is calibrated from the single p.e. region to that corresponding to 300 p.e.

Acknowledgements

We would like to acknowledge useful suggestions made by Professors W.R. Binns and P.C.

Gibbons. This work was supported by NIH grant R01 CA57222.

Appendix A. Model used for the fitting of the PMT response function

The pedestal response $f_0(q - q_p)$ in Eq. (2) was assumed to be a simple Gaussian

$$f_0(q - q_p) = \frac{1}{\sqrt{2\pi}\sigma_p} e^{-1/2(q - q_p)/\sigma_p)^2}. \quad (\text{A.1})$$

For the ideal (noiseless) single p.e. response $f_1^0(q - q_p)$, we adopted a model given by Dossi et al. [2], basically assuming that the single p.e. response consists of exponential and Gaussian parts

$$f_1^0(q - q_p) = H(q - q_p) \left[\frac{(p_E)}{C} e^{-(q - q_p)/C} + \frac{(1 - p_E)}{g_N} \frac{1}{\sqrt{2\pi}\sigma_0} e^{-1/2((q - q_p - q_0)/\sigma_0)^2} \right]. \quad (\text{A.2})$$

In this response, $H(q - q_p)$ denotes the Heaviside function, p_E is the fraction of events associated with the exponential component, C determines the decay of the exponential part, q_0 is the mean and σ_0 standard deviation of the Gaussian part and the factor

$$g_N = \frac{1}{2} \left[1 + \text{Erf} \left(\frac{q_0}{\sqrt{2}\sigma_0} \right) \right]$$

is the normalization for the truncated Gaussian.

In the absence of the saturation effects, the photomultiplier's response to multiple p.e.'s is a convolution of single p.e. responses and can be written as a simple recursive relation

$$f_n^0(q - q_p) = f_{n-1}^0(q - q_p) \otimes f_1^0(q - q_p). \quad (\text{A.3})$$

While the double p.e. response function $f_2^0(q - g_p)$ can be derived analytically [2], for higher n , the derivation becomes intractable. The photomultiplier tube under investigation possesses an extremely high single p.e. resolution and the usual Gaussian approximation of the $f_n^0(q - q_p)$ for $n > 2$ poorly describes measured pulse-height distributions. The multiple p.e. response functions were instead calculated “on the fly”, during fitting, by the numerical convolution of Eq. (A.3). The final set of response functions $f_n(q - g_p)$ was calculated by numerically convolving ideal responses $f_n^0(q - g_p)$ with the pedestal noise (Eq. (A.1)):

$$f_n(q - g_p) = f_n^0(q - g_p) \otimes f_0(q - q_p). \quad (\text{A.4})$$

The procedure described is extremely computationally intensive but produces excellent agreement between the measured data and the fit.

References

- [1] A.G. Wright, Nucl. Instr. and Meth. A 433 (1999) 507.
- [2] R. Dossi, et al., Nucl. Instr. and Meth. A 451 (2000) 623.
- [3] T. Araki, H. Misawa, Rev. Sci Instrum. 66 (12) (1995) 5469.
- [4] F.S. Choa, et al., Appl. Phys Lett. 69 (24) (1996) 3668.
- [5] A. Fyodorov, et al., Nucl. Instr. and Meth. A 413 (1998) 352.
- [6] A. Kilpelä, J. Kostamovaara, Rev. Sci. Instrum. 68 (6) (1997) 2258.
- [7] P. Marciniwski, Licentiate Thesis, Uppsala University, 1997.
- [8] E.H. Bellamy, et al., Nucl. Instr. and Meth. A 339 (1994) 468.
- [9] I. Chirikov-Zorin, et al., Nucl. Instr. and Meth. A 456 (2000) 310.
- [10] R. Perrino, et al., Nucl. Instr. and Meth. A 457 (2001) 571.
- [11] A.G. Wright, IEEE Trans. Nucl. Sci. NS-34 (1) (1987) 414.